IET Communications

Research Article

Journals
The Institution of Engineering and Technology

REC

Waveform design for radar-embedded communications exploiting spread spectrum technology

ISSN 1751-8628
Received on 2nd October 2015
Revised on 3rd April 2016
Accepted on 29th April 2016
doi: 10.1049/iet-com.2015.0936
www.ietdl.org

Baoguo Li, Jing Lei ✉, Wei Cao, Lei Wen, Yuheng Mou

School of Electronic Science and Engineering, National University of Defense Technology, Changsha, Hunan Province, People's Republic of China, 410073

✉ *E-mail: leijing@nudt.edu.cn*

REC

Abstract: Radar-embedded communication (REC) provides a reliable and low probability of intercept (LPI) communication link to the intended receivers while masking its presence from intercept receivers. This study summarises all the waveform design schemes as well as receiver processing strategies for intra-pulse REC, which forms the communication symbol waveform during one pulse interval and utilises de-correlation processing on the receiver side. Based on the set of eigenvectors after eigen-decomposition of sampled radar waveform, three design approaches are considered: 1 eigenvectors-as-waveforms, 2 weighted-combining and 3 dominant-projection (DP). Specifically, DP performs better than the other two approaches even in multipath environment by using one projection matrix masked random vector to represent a communication symbol. Aimed by the drawbacks of DP, the authors propose a novel waveform generation approach called modified DP (MDP) in this study. MDP uses a common digitally-modulated communication symbol spread by a pseudorandom sequence, so that it can enlarge the Euclidean distances between different data symbols and generate soft information for soft decision decoding, thus improving symbol error ratio and bit error ratio. Simulation results show that MDP significantly improves the reliability performance especially when channel coding is used, while also maintaining a relatively equal anti-intercept performance.

MDP: modified DP

1 Introduction

Low probability of interception (LPI) communication technologies have drawn considerable interests in both military and civil applications due to their secure nature against the intercept receivers. Nicholson has described four sequential operations that intercept receiver attempt to perform in [1], i.e. to cover, detect, intercept or exploit the signals. LPI communication technologies mean that the waveforms of communication systems must be specially selected and designed to combat the malicious attempts of intercept systems. Generally speaking, the waveforms should have those characteristics as follows:

Low probability of cover (LPC): It is aimed to increase the degree of difficulty for the unintended receivers to cover the signal in time, frequency and spatial domains. In civil communications, physical layer security makes the eavesdroppers initially lie on SNR-disadvantageous areas by exploiting spatio-temporal characteristics of wireless channels [2], such as beam-forming and artificial noise injection. However, much work has to be conducted before the practical application of those techniques in electronic systems. While in military communications, traditional covert communication employs signal's uncertainty in time, frequency and space domains by using time-hopping, frequency hopping and extremely narrow beam, respectively.

Low probability of detection (LPD): It is aimed to reduce the feasibility of the unintended receivers to judge whether useful signals exist in the covered receiving signals or not. Hence, concealing an emitter's location may require that the transmit signal should satisfy the LPD property. Direct sequence spread spectrum system is an example of LPD due to its extremely low signal power.

Low probability of interception: It is aimed to deny an unintended intercept receiver so that any features of transmitted signal cannot be extracted to distinguish the signals, such as noise communications [3, 4]. In a noise communication system, the input message is multiplied by a noise source. Meanwhile, the noise source is transmitted to the receiver side over another channel, which is called transmit reference technology. The receiver uses the noise source to demodulate the signal and retrieve the message. In frequency domain, as noise communication signal looks like normal communication signal, intercept receiver can easily detect the signal [4]. However, due to the noise-like characteristics, intercept receiver cannot extract the signal type. If the intercept receiver judges it as an important signal, large power jamming may be used to cover the occupied frequency bandwidth.

Low probability of exploitation (LPE): It is aimed to furnish the communication signals with the ability to reduce the unintended receiver's probability of successful message recovery operations, otherwise it may affect the communicators adversely. Signal that increases the difficulty of this type of exploitation is assumed to hold the property of LPE, e.g. encryption.

According to the aforementioned analyses, LPD is safer than LPI and LPE due to its inherent covertness which is immune to jamming. It seems to be a feasible LPD solution to hide communication signal in other electromagnetic radio such as radar signal, which is so-called radar-embedded communications (REC).

As is shown in Fig. 1*a*, radar illuminator, a friend or foe, can help to detect whether there exists some desired information or not in a given area. The task of REC is burdened by a tag, which is triggered by the radar signal and subsequently processes the received signal and retransmits the processed signal towards the desired receiver. During the process, useful information is embedded into the normal radar backscatter as a mask. The intended receiver can extract the communication information while intercept receiver fails, for that the former possesses the prior information of the embedded signal while the latter does not. Spectrum of the hidden communication signal occupies the

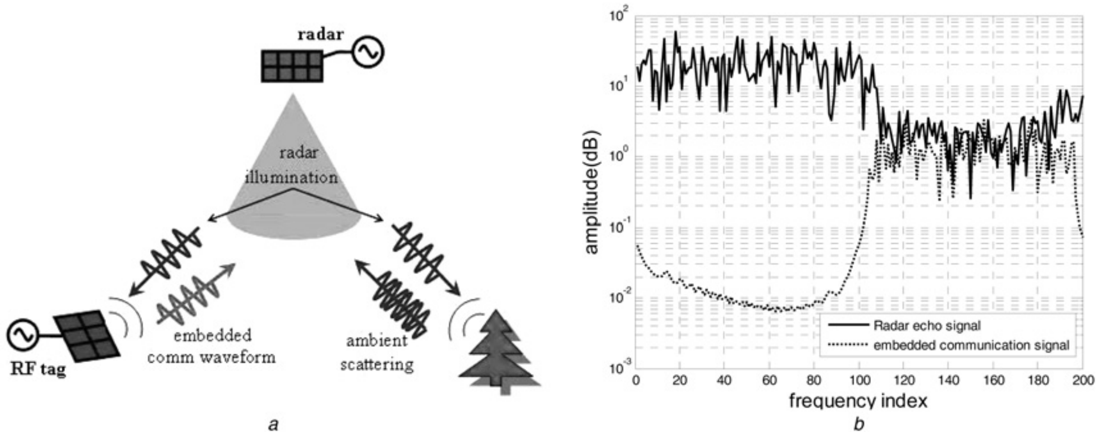

Fig. 1 *Paradigm and spectrum behaviour of REC system*

a Paradigm of REC (From [5])
b Spectrum of radar echo signal and embedded communication signal

stop-band of radar echo signal spectrum, which is illustrated in Fig. 1*b*. Therefore, an intercept receiver can only discover the radar signals [6] other than realise the existence of covert communication signal.

The earliest approaches in REC [7–11] are so-called inter-pulse REC. It mainly utilised radar illumination consisting of numerous of pulses as is encountered in synthetic aperture radar applications, and carrying information amongst the pulses. Inherited from the inter-pulse modulation, intra-pulse waveform is designed to hide the information, which improved the data rate and enhanced the covert performance meanwhile [6, 12–15]. Communication is accomplished by re-modulating the incident radar waveform into one of some set of communication waveforms during one pulse interval. It is studied in [6] to optimally design the communication waveforms to jointly provide a high communication performance at the receiver while maintaining a relative similar LPI performance against eavesdroppers.

Three waveform design methods are proposed, i.e. eigenvectors-as-waveforms (EAW), weighted-combining (WC) and dominant-projection (DP) [6]. DP's performance is proved to be superior to the other two methods. The processing gain and LPI metric of DP approach are obtained through theoretical analysis [13, 14]. In DP approach, each communication symbol is represented by a random vector multiplied by a projection matrix to guarantee the covertness, the intended receiver uses the same random vector to match the received signal and make the symbol decision through correlation. In this paper, an improved waveform is proposed which exploits a common phase shift keying symbol spread by a pseudorandom sequence to represent a symbol. Compared to the DP, our method's symbol error ratio (SER) performance is greatly improved while LPI performance is not degraded. Another advantage is that channel coding with soft decision can be used in our method to further decrease the bit error ratio (BER).

The rest of the paper is organised as follows. The REC waveform and receiver design is introduced in Section 2. In Section 3, principles of our method are illustrated and the LPI performance metric is also deduced. Simulation results are given in Section 4 and concluding remarks are finally made in Section 5.

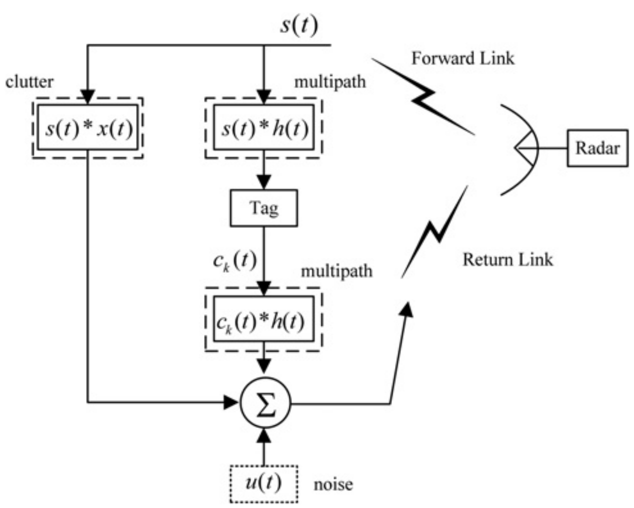

Fig. 2 *REC time signal model*

2 Signal model and communication design

2.1 Signal model and DP approach

As shown in Fig. 2, REC system work as an integrated communication system with a forward and return link. In the forward link, radar transmit signal $s(t)$, which is absorbed by both the tag and radar target. While in the return link, on one hand, target reflects the radar signal as radar echo or clutter; on the other hand, the tag re-modulates the radar signal incorporating the information intended to transfer.

Suppose the tag will transmit one of K communication symbols to the desired receiver. The kth transmitted communication symbol is defined as $c_k(t)$. The received signal is then given as

$$y(t) = s(t) * x(t) + \alpha c_k(t) * h(t) + u(t) \tag{1}$$

where the clutter process is $x(t)$, multipath channel response is denoted as $h(t)$, thermal noise is represented by $u(t)$, and α is an attenuation constant.

Typically, receiver oversamples the received signal by some amount greater than Nyquist sampling rate. let N be the number of samples required to sufficiently represent the incident radar illumination according to the Nyquist criterion for the half-power bandwidth (thus N is the time-bandwidth product) and let M be the additional factor by which the waveform is over-sampled (to facilitate sufficient degrees of freedom for symbol design) [14]. The sampled radar waveform is denoted as the length of $\boldsymbol{NM}$ vectors and the discrete clutter profile is x. When considering the convolution of s, it should be noticed that there are $2\boldsymbol{NM}-1$ possible shifts of s. Therefore, define the $\boldsymbol{NM} \times (2\boldsymbol{NM}-1)$

Toeplitz matrix $\boldsymbol{S}$ as

$$\boldsymbol{S}=\begin{bmatrix} s_{NM-1} & s_{NM-2} & \cdots & s_0 & 0 & \cdots & 0 \\ 0 & s_{NM-1} & \cdots & s_1 & s_0 & \cdots & 0 \\ \vdots & \vdots & \ddots & \vdots & \vdots & \ddots & \vdots \\ 0 & 0 & \cdots & s_{NM-1} & s_{NM-2} & \cdots & s_0 \end{bmatrix} \tag{2}$$

Discarding the multipath, the signal received by the radar can be expressed as

$$\boldsymbol{y}=\boldsymbol{S}x+\alpha \boldsymbol{c}_k+\boldsymbol{u} \tag{3}$$

where $\boldsymbol{c}_k$ is a length $\boldsymbol{NM}$ discretised version of the communication symbol and $\boldsymbol{u}$ is a length $\boldsymbol{NM}$ vector of AWGN noise samples.

Communication waveforms can be obtained by computing the eigen-decomposition of the correlation of $\boldsymbol{S}$ as

$$\boldsymbol{S}\boldsymbol{S}^{\mathrm{H}}=\boldsymbol{V}\boldsymbol{\Lambda}\boldsymbol{V}^{\mathrm{H}} \tag{4}$$

where $\boldsymbol{V}=[\boldsymbol{v}_0\ \boldsymbol{v}_1\ \cdots\ \boldsymbol{v}_{NM-1}]$ contains $\boldsymbol{NM}$ eigenvectors, $\boldsymbol{\Lambda}$ is a diagonal matrix comprised of the associated eigenvalues, and $(\cdot)^{\mathrm{H}}$ is the Hermit operator. Based on the eigen-decomposition, three waveform design methods are described as follows.

Eigenvectors-as-waveforms. EAW directly utilises some amount of non-dominant eigenvectors as waveforms, $\boldsymbol{c}_k=\boldsymbol{v}_k$, $k=1, 2, \ldots, K$, selecting the eigenvectors corresponding to the K smallest eigenvalues.

Weighted-combining (WC). The WC waveform is $\boldsymbol{c}_k=\tilde{\boldsymbol{V}}_{\mathrm{ND}}\boldsymbol{b}_k$, $\tilde{\boldsymbol{V}}_{\mathrm{ND}}=[\boldsymbol{v}_0\boldsymbol{v}_1\cdots\boldsymbol{v}_{L-1}]$, where each $\boldsymbol{b}_k$ is a different weight vector which is only known to the tag and the intended receiver.

Dominant-projection (DP). Separating the eigenspace into dominant and non-dominant subspaces allows the partitioning of the eigen-decomposition of (4) as

$$\boldsymbol{S}\boldsymbol{S}^{\mathrm{H}}=\boldsymbol{V}\boldsymbol{\Lambda}\boldsymbol{V}^{\mathrm{H}}=\left[\boldsymbol{V}_{\mathrm{D}}\ \boldsymbol{V}_{\mathrm{ND}}\right]\begin{bmatrix} \boldsymbol{\Lambda}_{\mathrm{D}} & 0 \\ 0 & \boldsymbol{\Lambda}_{\mathrm{ND}} \end{bmatrix}\begin{bmatrix} \boldsymbol{V}_{\mathrm{D}}^{\mathrm{H}} \\ \boldsymbol{V}_{\mathrm{ND}}^{\mathrm{H}} \end{bmatrix} \tag{5}$$

where V_{D} is an $\boldsymbol{NM}\times m$ matrix of the m dominant eigenvectors, and V_{ND} is of dimension $\boldsymbol{NM}\times(\boldsymbol{NM}-m)$ and consists of the non-dominant eigenvectors. The parameter m represents the proportion of dominant and non-dominant space, called projection index. Similarly, $\boldsymbol{\Lambda}_{\mathrm{D}}$ is a $m\times m$ diagonal matrix of the m dominant eigenvalues, and $\boldsymbol{\Lambda}_{\mathrm{ND}}$ is the $(\boldsymbol{NM}-m)\times(\boldsymbol{NM}-m)$ diagonal matrix of non-dominant eigenvalues.

The DP method projects a seed vector (of dimensionality $\boldsymbol{NM}$) away from the dominant subspace as a whole. To project away from the dominant subspace, the projection matrix

$$\boldsymbol{P}=\boldsymbol{I}-\boldsymbol{V}_{\mathrm{D}}\boldsymbol{V}_{\mathrm{D}}^{\mathrm{H}}=\boldsymbol{V}_{\mathrm{ND}}\boldsymbol{V}_{\mathrm{ND}}^{\mathrm{H}} \tag{6}$$

is used to form the kth communication symbol as

$$\boldsymbol{c}_k=\boldsymbol{P}\boldsymbol{b}_k \tag{7}$$

The vector $\boldsymbol{b}_k$ is a pseudo-random seed that is known to both the desired receiver and the tag. DP approach has been proved to be better than the other two methods in terms of communication performance, covertness, and robustness to multipath [6]. Therefore, only the DP approach is considered in this paper.

2.2 Receiver design

In intra-pulse REC systems, an intended receiver can extract the embedded information by determining the most possible communication waveforms using the waveform set stored offline. Without prior knowledge of possible waveform, an eavesdropper will keep guessing if an embedded signal even exists among the masking interference, thereby maintaining the covert nature of the embedded signal. Three receive processing methods are considered in the literature as follows.

2.2.1 Matched filter (MF) receiver: In the MF detection [12] the receiver matches the received signal to one of the given set of waveforms that are possibly present, selecting the waveform of maximum correlation, which can be expressed as follows

$$\hat{k}=\arg\left\{\max_k\left\{\left|\boldsymbol{c}_k^{\mathrm{H}}\boldsymbol{y}\right|\right\}\right\} \tag{8}$$

where $\hat{k}$ is the index of the kth waveform. MF method does not perform well due to the fact that it cannot decorrelate the useful signal from the interference, which is the radar scatter signal.

2.2.2 Decorrelating-filter (DF) receiver: DF receiver does not require knowledge of relative power levels [12]. Appending the K communication waveforms to the Topelitz matrix $\boldsymbol{S}$, the $\boldsymbol{Nm}\times(2\boldsymbol{Nm}+k-1)$ matrix $\boldsymbol{C}$ can be formed as

$$\boldsymbol{C}=[\boldsymbol{S}\boldsymbol{c}_1\ldots\boldsymbol{c}_k] \tag{9}$$

which models all the possible signal components (including both radar and communication) that may exist in the received signal $\boldsymbol{r}$. The kth DF can thus be obtained as

$$\boldsymbol{w}_k=\left(\boldsymbol{C}\boldsymbol{C}^{\mathrm{H}}\right)^{-1}\boldsymbol{c}_k \text{ for } k=1, 2, \ldots K \tag{10}$$

DF receiver performs better than MF due to the fact that $\boldsymbol{w}_k$ de-correlates the waveform from the interference. The disadvantage of DF lies in that decorrelator enhances the noise especially at low SNR. Similar with MF, the decision is made by selecting the communication symbol that satisfies

$$\hat{k}=\arg\left\{\max_k\left\{\left|\boldsymbol{w}_k^{\mathrm{H}}\boldsymbol{y}\right|\right\}\right\} \tag{11}$$

2.2.3 Diagonally loaded decorrelating (DLD) receiver: DLD receiver is given in [13] as

$$w_k=(\boldsymbol{S}\boldsymbol{S}^{\mathrm{H}}+\delta\boldsymbol{I})^{-1}\boldsymbol{c}_k \text{ for } k=1, 2, \ldots, K \tag{12}$$

where $\delta=\lambda_{m+1}$ is the largest non-dominant eigenvalue. The diagonal loading can effectively prevent ill conditioning when $\boldsymbol{S}\boldsymbol{S}^{\mathrm{H}}$ is sparse. This filter reduces to

$$\begin{aligned} w_k &= (\boldsymbol{S}\boldsymbol{S}^{\mathrm{H}}+\lambda_{m+1}\boldsymbol{I})^{-1}\boldsymbol{c}_k=(\boldsymbol{V}\boldsymbol{\Lambda}\boldsymbol{V}^{\mathrm{H}}+\lambda_{m+1}\boldsymbol{V}\boldsymbol{V}^{\mathrm{H}})^{-1}\boldsymbol{c}_k \\ &\simeq \lambda_{m+1}^{-1}\boldsymbol{V}_{\mathrm{ND}}\boldsymbol{V}_{\mathrm{ND}}^{\mathrm{H}}\boldsymbol{b}_k=\lambda_{m+1}^{-1}\boldsymbol{c}_k \end{aligned} \tag{13}$$

The decision processing is the same with (11).

3 Novel method exploiting spread spectrum and soft decision decoding

3.1 Principle

According to the aforementioned analysis, we conclude that the basic mechanism of REC is to sample the radar waveform and form a mask matrix to hide the communication waveform. The common shortcomings of all the waveform generating and receive processing methods lie in that they just use hard decision, which decides the symbol by the matching result between received waveform and local waveform. In other words, these methods do not use the absolute value of the matching operation, which is actually very useful for the subsequent error correcting decoding. For the same channel codes, the gain of soft decision decoding is at least 2 dB higher than that of hard decision in AWGN channel. Second, Euclidean distances of different symbol waveform are not well designed, which will cause higher SER even that each symbol SNR is relatively high. In digital modulation theory, the SER does not only depend on the SNR but also the Euclidean distance of symbols.

In this section, we will propose a new waveform design method based on DP approach, namely modified DP (MDP), which combines traditional direct sequence spread and digital phase shift keying technology with DP.

The waveform generation and information embedding procedure are illustrated in Fig. 3*a*. Assume that $\boldsymbol{d}$ is a spread spectrum sequence of length $\boldsymbol{NM}$, which can be shortened by a pseudorandom sequence; the kth communication symbol can be expressed by

$$\boldsymbol{c}_k = \boldsymbol{P}\boldsymbol{b}_k \tag{14}$$

where $\boldsymbol{b}_k = \boldsymbol{d}\beta_k$, β_k is the constellation point of QPSK modulated symbol

$$\beta_k = \pm\sqrt{2}/2 \pm \sqrt{2}/2i \tag{15}$$

As shown in Fig. 3*b*, in the receiver side, we consider MF processing and DLD processing. MF processing can be expressed as

$$\mathrm{MF}_{\mathrm{output}} = \boldsymbol{c}_k^{\mathrm{H}}\boldsymbol{y} \tag{16}$$

and DLD processing can be expressed as

$$\mathrm{DLD}_{\mathrm{output}} = \boldsymbol{w}_k^{\mathrm{H}}\boldsymbol{y} \tag{17}$$

where $\boldsymbol{w}_k = (\boldsymbol{SS}^{\mathrm{H}} + \lambda_{m+1}\boldsymbol{I})^{-1}\mathbf{Pd}$ for $k = 1, 2, \ldots, K$, which combines the decorrelation and despread into one step. The result of (16) and (17) can be sent to channel decoder for soft decision decoding, while DP just decide which symbol the waveform belongs to and the decision result can only be used for hard decision when channel coding is used in the transmitter, as (8) and (11) shows.

3.2 Processing gain

The processing gain is defined as the ratio of the signal-to-interference-plus-noise ratios (SINR) at the input to and the output of receive processing. The processing gain of DP approach has been deduced under DLD receiving conditions [13, 14]. The receive filter of DP approach is $\boldsymbol{w}_k = (\boldsymbol{SS}^{\mathrm{H}} + \delta\boldsymbol{I})^{-1}\boldsymbol{c}_k$ for $k = 1, 2, \ldots, K$, which is related with each symbol. In MDP approach, $\boldsymbol{w}_k = (\boldsymbol{SS}^{\mathrm{H}} + \lambda_{m+1}\boldsymbol{I})^{-1}\mathbf{Pd}$ for $k = 1, 2, \ldots, K$, which is independent with symbol. Therefore, the deducing procedure of MDP approach is slightly different from the DP approach. Detailed procedure is given in the appendix. Final result can be expressed as

$$\Delta(m) = \frac{\boldsymbol{NM}(\boldsymbol{NM} - m)(\sigma_x^2 + \sigma_u^2)}{\sigma_x^2\,\mathrm{tr}\{\boldsymbol{\Lambda}_{\mathrm{ND}}\} + \sigma_u^2(\boldsymbol{NM} - m)} \tag{18}$$

where σ_x^2 and σ_u^2 are the variance of clutter and noise, respectively. From (18), we can see that the processing gain is exactly the same with DP's [13, 14].

Metcalf *et al.* [13] gives some simple forms of (18), which are shown as follows.

Noise dominant case: $\sigma_u^2 \gg \sigma_x^2$ (i.e. the noise power is much greater than the clutter power), then (18) results in $\Delta(m) \simeq \boldsymbol{NM}$, called coherently integration gain.

Clutter dominant case: $\sigma_x^2 \gg \sigma_u^2$ (i.e. the clutter power is much greater than the noise power), then (18) simplifies to $\Delta(m) \simeq \boldsymbol{NM}\lambda_{m+1}^{-1}$. Small values of λ_{m+1} ensure the processing gain becomes much greater than the coherent integration gain (NM). Table 1 show the processing gain of clutter dominant case, where N equals to 2 and M equals to 100 for LFM signal. It can be seen that the gain increase monotonically with projection index m, while increase even faster when m is in the transitional region and non-dominant region.

3.3 Euclidean distance of different waveforms after processing

The SER of digital modulation depends on both the SNR of single symbol and Euclidean distance between different waveform sent to the demodulator. The Euclidean distance of DP waveform was not well designed because DP just use a random vector multiplied by a mask matrix.

The DLD filter uses a decorrelating processing $(\boldsymbol{SS}^{\mathrm{H}} + \lambda_{m+1}\boldsymbol{I})^{-1}$ appended by the MF filter, which is independent with symbol. Hence, for convenience, we take MF method as an example to deduce the Euclidean distance of each symbol after processing, and the symbol is constrained to be QPSK modulated.

For both DP and MDP approaches, the normalised power is restricted to 1, which is $\|\boldsymbol{b}_k\|^2 = 1$. For MDP approach, the Euclidean distance after processing is $|(\mathbf{Pd})^{\mathrm{H}}\mathbf{Pd}(\beta_k) - (\mathbf{Pd})^{\mathrm{H}}\mathbf{Pd}(\beta'_k)|$, β_k and β'_k are different QPSK symbols as (15), hence

$$\begin{aligned}&\left|(\mathbf{Pd})^{\mathrm{H}}\mathbf{Pd}(\beta_k) - (\mathbf{Pd})^{\mathrm{H}}\mathbf{Pd}(\beta'_k)\right|\\&= \sqrt{2}\left|(\mathbf{Pd})^{\mathrm{H}}\mathbf{Pd}\right|\\&= \sqrt{2}(\boldsymbol{NM} - m)/\boldsymbol{NM}\end{aligned} \tag{19}$$

Detailed mechanism can also be seen in appendix.

For DP approach, the Euclidean distance after processing can be expressed as

$$E(|\boldsymbol{c}_k^{\mathrm{H}}\boldsymbol{c}_k - \boldsymbol{c}_k^{\mathrm{H}}\boldsymbol{c}'_k|) \cong (\boldsymbol{NM} - m)/\boldsymbol{NM} \tag{20}$$

where $\boldsymbol{c}_k$ and $\boldsymbol{c}'_k$ are different symbol waveform, which is not correlated with each other. From (19) and (20), we can see that the distance is $\sqrt{2}$ times than that of DP approach. Therefore, under the same SINR, it is expected that the SER of MDP approach is better than that of DP approach. For constant PSK modulation in AWGN channel, SER has deterministic relationship with SNR and Euclidean distance. While in REC systems, the clutter and noise mixed together after decorrelation and consequently cannot be treated as white Gaussian noise. Hence in Section 4, we will simulate the MDP approach.

3.4 Computing of log likelihood ratio (LLR) for soft decision

It is necessary to provide the corresponding LLR of each symbol for the soft decision decoding. To get the LLR, we should obtain the clutter and noise power after DLD processing, which are given in appendix as

$$R_o = \delta^{-2}\sigma_x^2\mathrm{tr}\{\boldsymbol{\Lambda}_{\mathrm{ND}}\}/\boldsymbol{NM} \tag{21}$$

$$N_o = \delta^{-2}\sigma_u^2(\boldsymbol{NM} - m)/\boldsymbol{NM} \tag{22}$$

The LLR is the logarithm ratio of probabilities of a 0 bit being transmitted against a 1 bit being transmitted for received signal. The LLR for a bit b is defined as

$$L(b) = \log\left[\frac{\Pr(b = 0|r = (x, y))}{\Pr(b = 1|r = (x, y))}\right] \tag{23}$$

Assuming equal probability for all symbols, the LLR over AWGN

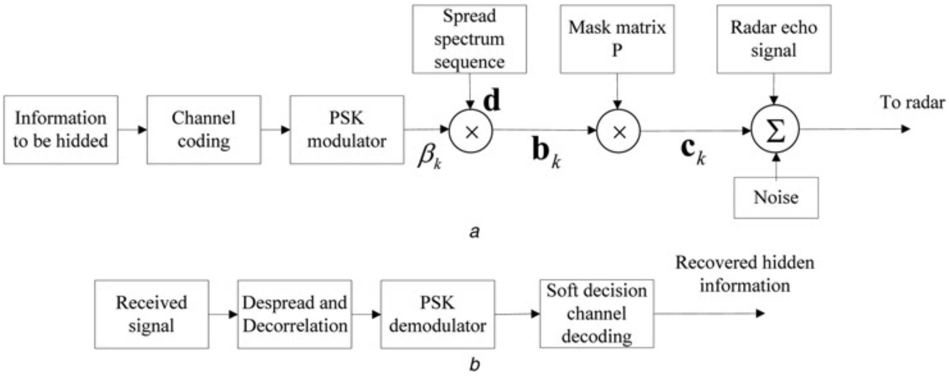

Fig. 3 *Block diagram of transmitter and receiver of REC system exploiting MDP*

a Block diagram of generating embedded singnal

b Block diagram of recovering the embedded signal

channel can be expressed as

$$L(b) = \log\left[\frac{\sum_{s\in S_0} \mathrm{e}^{-(1/\sigma^2)\left((x-s_x)^2+(y-s_y)^2\right)}}{\sum_{s\in S_1} \mathrm{e}^{-(1/\sigma^2)\left((x-s_x)^2+(y-s_y)^2\right)}}\right] \qquad (24)$$

where r is the received signal with coordinates (x, y). b is the transmitted bit (one of the K bits in an M-ary symbol, assuming all M symbols are equally probable). S_0 is the ideal symbol or constellation point with bit 0, at the given bit position. S_1 is the ideal symbol or constellation point with bit 1, at the given bit position. s_x is the in-phase coordinate of ideal symbol or constellation point. s_y is the quadrature coordinate of ideal symbol or constellation point. σ^2 is the noise variance of baseband signal. Here we consider $\sigma^2 = R_o + N_o$ for LLR calculation, which is the sum of noise and clutter power after processing.

3.5 Intercept metric

The ability of an intercept receiver to detect the presence of a REC symbol depends on many factors, such as the time-width and bandwidth of the communication waveform, which must be known to the desired receiver and is not available to the intercept receiver. For all LPI metrics, the intercept receiver is assumed to have knowledge of the time-width and bandwidth used by the REC system. This knowledge provides a 'worst case' scenario, and should bound the performance of an intercept receiver.

3.5.1 Normalised correlation: An LPI metric was established in [6] that measures normalised correlation to quantify the covert nature of the embedded communication symbol. This metric in effect 'scans' the eigenspace of the radar waveform by systematically projecting away the hypothesised dominant subspace from the received signal and examining the normalised correlation between each possible communication symbol and the residue of the projection. In other words, for $\tilde{m} = 1, 2, \ldots, \boldsymbol{NM}$, define the hypothesised dominant subspace as the $\boldsymbol{NM} \times \tilde{m}$ matrix $\tilde{\boldsymbol{V}}_{\mathrm{D},\tilde{m}}$ composed of the eigenvectors corresponding to the $\tilde{m}$ largest eigenvalues. Therefore, to project away from this subspace, form a projection matrix as

$$\boldsymbol{P}_{\tilde{m}} = \boldsymbol{I} - \tilde{\boldsymbol{V}}_{\mathrm{D},\tilde{m}}\tilde{\boldsymbol{V}}_{\mathrm{D},\tilde{m}}^{\mathrm{H}} = \tilde{\boldsymbol{V}}_{\mathrm{ND},\tilde{m}}\tilde{\boldsymbol{V}}_{\mathrm{ND},\tilde{m}}^{\mathrm{H}} \qquad (25)$$

Applying $\boldsymbol{P}_{\tilde{m}}$ to the discretised received signal at time sample ℓ, the $\tilde{m}$th residual is obtained as

$$z_{\tilde{m}}(\ell) = \boldsymbol{P}_{\tilde{m}} y(\ell) \qquad (26)$$

This residue is then correlated with the kth communication symbol as [6]

$$\eta_{k,\tilde{m}}(\ell) = \frac{\left|c_k^{\mathrm{H}} z_{\tilde{m}}(\ell)\right|}{\sqrt{(c_k^{\mathrm{H}} c_k)(z_{\tilde{m}}^{\mathrm{H}}(\ell) z_{\tilde{m}}(\ell))}} \qquad (27)$$

The normalised correlation gives an idea of the accuracy with which the eavesdropper can detect the transmitted waveforms; therefore it can be used as an LPI metric. The efficacy of this metric was examined in [16]. It appears that there is a limit to the efficacy of this metric when dealing with multipath scenes. Therefore, an improved metric is needed to quantify the LPI nature.

3.5.2 SNR gap: For both DP and MDP, it is necessary to deal with the null hypotheses of no transmitted symbol for MDP method. That is to say, we need to detect whether the symbol is present or not during the pulse duration, which can use Neyman Pearson critrion as in [13]. The difference with DP lies in that MDP first makes a decision whether a symbol is present or not, according to that the output of (17) exceeds the decision threshold or not, which is computed by the false alarm probability in (27) of [13]. If a symbol is present, the output is further demodulated based on the Euclidean distance between the constellation point and itself.

Despite the fact that both intended receiver and intercept receiver attempt to detect the signal, the probability of detection and interception are different under the same SNR condition due to the asymmetry of prior information owned by them. In other words, to get the same probability of discovering signal, the SNR needed by intercept receiver must be higher than the intended receiver to compensate the disadvantageous non-cooperation. Hence we select the difference of SNR values between them, i.e. SNR gap, as another LPI metric. It is expected that the greater SNR gap is, the better LPI performance is.

Table 1 Processing gain-clutter dominant ($N = 2$, $M = 100$)

m	10	30	50	70	80	90	100	110	130	150	170	190
Gain, dB	19.4	19.8	20.0	20.3	20.5	21.0	26.0	31.6	39.1	43.0	45.0	45.9

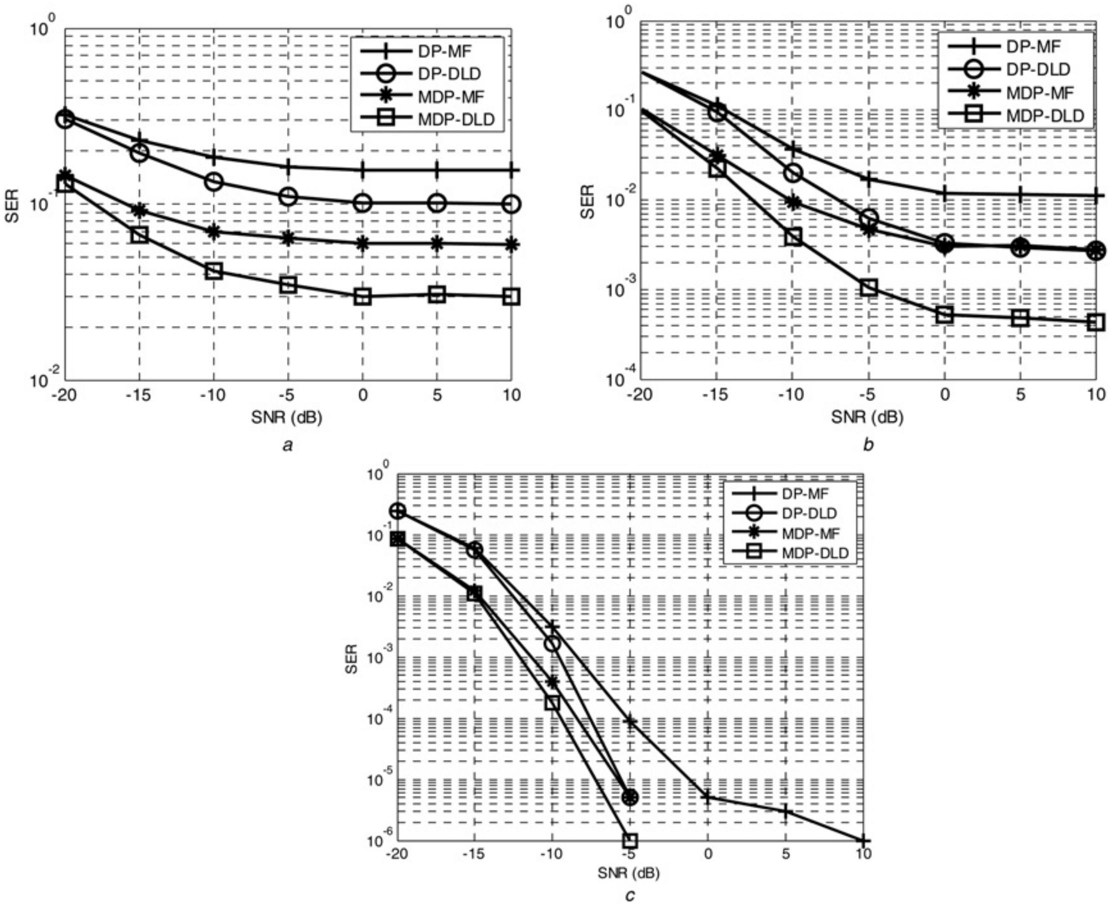

Fig. 4 *SER against SNR (m = 110)*

a SIR −35 dB
b SIR −30 dB
c SIR −25 dB

4 Computer simulations and performance

Simulations in this section are performed considering the radar illumination waveform as the LFM signal, whose sampled version is $s(n) = e^{j(\pi/N)n^2}$, where N is the length of waveform transmitted and $n = [0, 1 \ldots, N-1]$.

4.1 SER performance

In this section, we compare the SER of MDP approach with DP approach, using MF and DLD receive processing, respectively. In Section 3, we have proved that the processing gain of MDP approach is identical to that of DP approach while the Euclidean distance is larger than that of DP. In simulation, we can see if it is true that Euclidean distance will affect the SER. In the simulation, the oversample factor is 2, and N equals to 100, the projection index m is 110 or 150. The SNR is from −20 to 10 dB with a step of 5 dB, and SIR is set to −35, −30 and −25 dB. Monte–Carlo simulations are performed for over 1,000,000 trials and then SER curves are plotted. Simulation can be divided into two cases as follows.

Case 1: $m = 110$. The curves are plotted in Figs. 4*a*–*c*. At SIR −35 dB, for both MF and DLD processing, the curves are flat. In this case, clutter power is larger than noise power, so the gain is plotted in Table 1. According to Table 1, the gain is 31.6 dB for $m = 110$, so the SINR after processing is about $(-35 + 31.6) = -3.4$ dB, this is the reason why the curves are flat. At SIR −30 dB, with the increasing of SNR, DP-DLD and MDP-MF coincided, while MDP-DLD is better than all the other method, which is of 15 dB gain over other methods at the BER $5{*}10^{-3}$. At SIR −25 dB, it is the same with that of −30 dB that MDP-MF coincides with DP-DLD. At BER of 10^{-4} and 10^{-5}, MDP-DLD both outperforms DP-DLD with 1.5 dB, and outperforms MDP-MF with 4 and 6 dB, respectively.

Case 2: $m = 150$. The curves are plotted in Figs. 5*a*–*c*. Compared with the case of $m = 110$, the performance is significantly improved at all SIR values and there is no difference between MF and DLD processing, which means these two curves almost coincides. This is due to the fact that when m is larger, the entry $\lambda_{m+1}^{-1}\boldsymbol{I}$ in (13) is larger than $\boldsymbol{SS}^{\mathrm{H}}$ and the decorrelate vector $\boldsymbol{w}_k$ is close to $\lambda_{m+1}^{-1}c_k$, which is the same with MF. When SIR is −35 dB, both DP and MDP curves are flat, MDP approach can reach a SER of 10^{-3}, which greatly outperforms $m = 110$ at the range of $10^{-2}{\sim}10^{-1}$. When SIR is −30 dB and −25 dB, both DP and MDP decrease rapidly and are no longer flat. MDP outperforms DP of 3–5 dB at all SER. The performance difference between $m = 110$ and $m = 150$ is related to the fact that the processing gain of $m = 150$ is larger than that of $m = 100$ according to (18) and Table 1.

From the above, Monte–Carlo simulation results corroborate our analysis that MDP approach is far superior to DP approach at all SIRs and projection index values due to the larger Euclidean distances after receiver processing. For both MDP and DP approaches, DLD outperforms MF processing with relative low projection index. With the increase of projection index, the processing gain increases as Table 1 in the clutter dominant case, therefore the SER decreases. For relatively high projection index, SER performance of DLD is almost the same with that of MF.

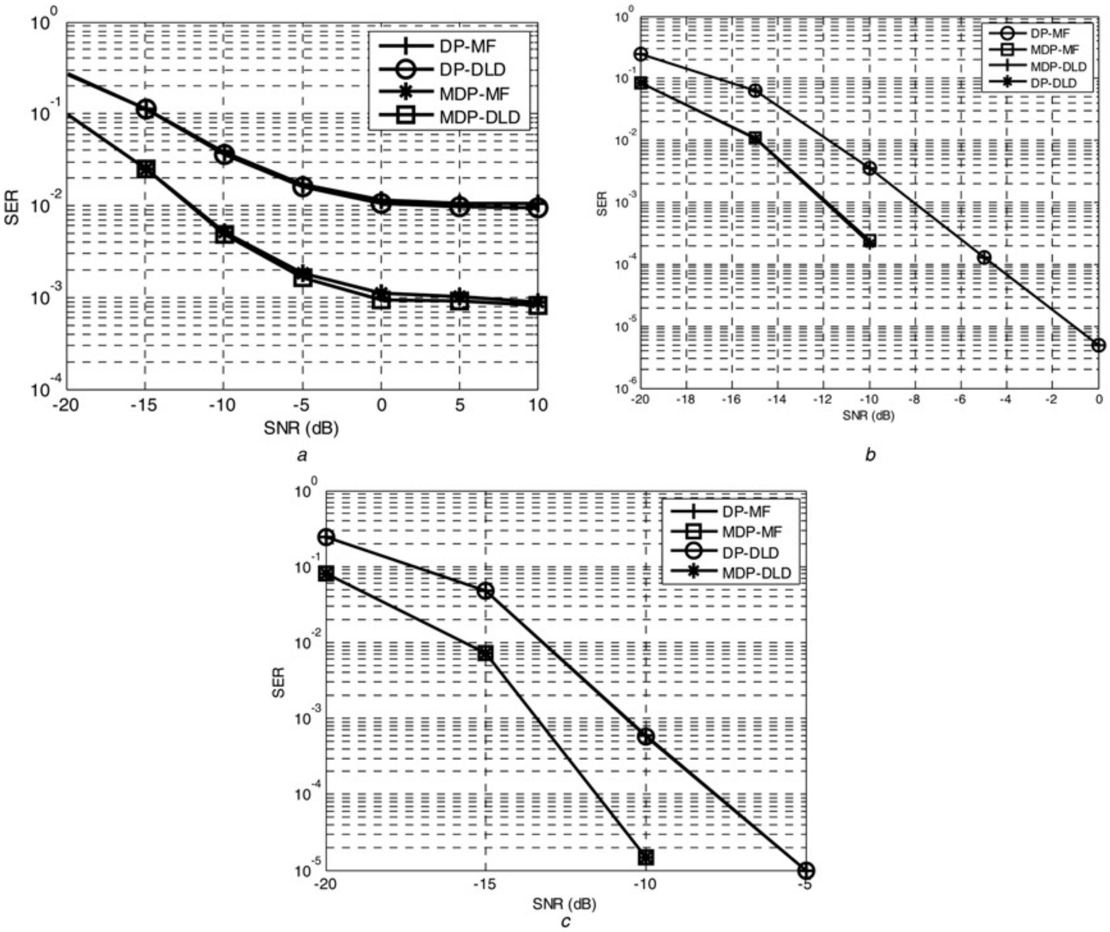

Fig. 5 *SER against SNR (m = 150)*

a SIR −35 dB
b SIR −30 dB
c SIR −25 dB

4.2 Channel coding performance

In this section, we will simulate the performance of channel coding for MDP approach. We use a convolutional code with the parameter of [1, 2, 7] for the channel coding unit as shown in Fig. 3, which means a code rate of 1/2 and constrained length of 7. According to information theory, for convolutional codes, the gain of soft decision decoding is about 2 dB higher than that of hard decision.

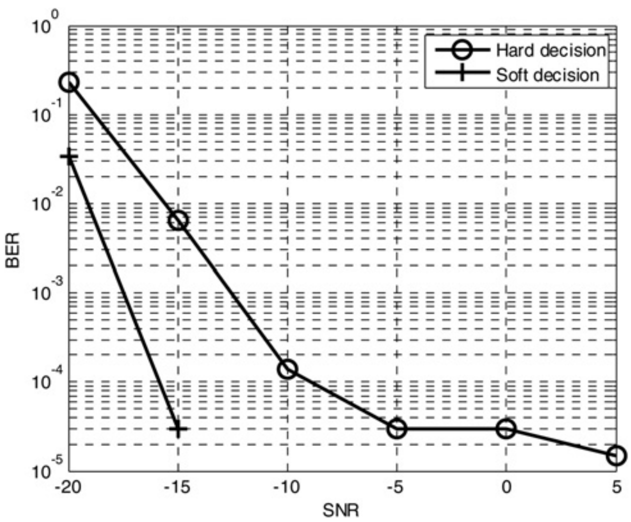

Fig. 6 *BER of hard decision and soft decision (−35 dB SIR, m = 110)*

In MDP-DLD, to test the BER, we should use a huge amount of trials. In order to reduce the computation load, we choose SIR −35 dB, whose SER is 10^{-2} to 10^{-1}, which is relatively high so that the Monte-Carlo times can be reduced. As shown in Fig. 6, we can see that at BER of 10^{-4} and 10^{-5}, the gain is 5 and 20 dB, respectively, which is much better than that of AWGN channel. This is due to the fact that channel after decorrelation cannot be treated as a simple AWGN channel, therefore, the gain of soft decision to hard decision is even higher when the channel is even worse.

4.3 LPI metric

MDP and DP are different just in symbol design aspect, both the desired receiver and intercept receiver detect the signal using a similar way, so the LPI performance of MDP and DP can both be evaluated using the metrics in Section 3.5.

The left-hand side of Fig. 7 illustrates the normalised correlation metrics of DP and MDP approach. The radar parameters are the same with the above, with a constant SIR of −35 dB and SNR of −5 dB. It can be seen that the maximum correlation is at about $m = 110$ with a value of just 25%. As such, we may infer that an intercept receiver, presumed to possess no prior knowledge of the set of embedded communication waveforms, would have virtually no ability to determine either the presence of these waveforms or their properties. It is also observed that the LPI performance of the DP and MDP approaches are quite similar from the view of normalised correlation metric.

In the simulation of SNR gap, we select an alternate LPI metric as detection statistics, which is described in (36) of [13]. Using $P_{fa} =$

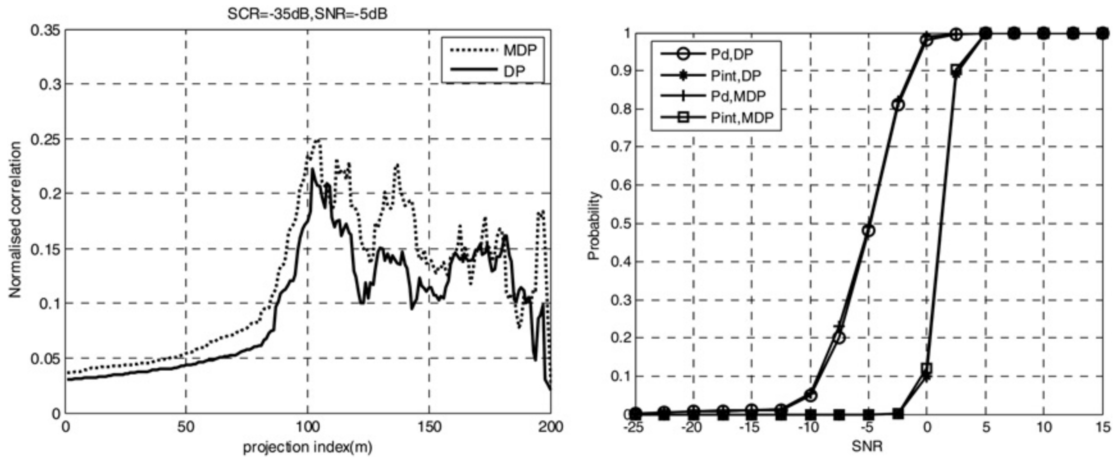

Fig. 7 *LPI metrics of DP and MDP. Left-hand side Normalised correlation; right-hand side SNR gap*

10^{-5}, the threshold for the intercept receiver as a function of n was calculated using (27) of [13]. Using this result, a Monte–Carlo simulation of 10,000 trials was run and the subsequent intercept probability P_{int} compared to the P_{d} results obtained by the two-stage detector. The diagonal loading term λ_{m+1} was chosen to be $m = 160$, with $N = 100$; $M = 2$. The clutter-to-noise ratio was set to 30 dB. The Neyman Pearson detector for the two-stage detector was also set to have $P_{fa} = 10^{-5}$. From the right-hand side of Fig. 7, it is observed that, for both DP and MDP, at the 50% mark, P_{int} is about 5 dB worse than the value of P_{d} for the two-stage detector, which means that the SNR gap is 5 dB.

From simulations of the above metrics, it is observed that the LPI performance of the DP and MDP approaches are quite similar, which is to be expected as they both utilise the same space for communication waveform design. That is to say, MDP approach does not decrease its LPI performance relative to DP even using the same spread spectrum sequence for each symbol. This is due to the fact that communication waveforms of MDP are still correlated with the mask radar scatter signal and the intercept receiver has no prior knowledge of the spread spectrum sequence.

5 Conclusions/outlook

Intra-pulse RECs have been summarised in waveform design and receiver design. A novel waveform design strategy and issues for intra-pulse RECs have been considered, and they result in a communication performance increase over previous intra-pulse DP schemes. Our method uses direct sequence spread and soft decision channel coding to replace the random vector waveform of DP. It can maintain relative equal LPI performance with DP approach while decrease the SER and BER at the same SNR due to the increase of Euclidean distance and utilisation of soft decision decoding. Future work in this regard will focus on practical implementation issues as well as means to expand the waveform design space in order to achieve even higher data-rates. Furthermore, it can use different spread spectrum sequence for different symbol waveform to further enhance the covertness at the cost of a little increase of system load.

6 Acknowledgments

This work was supported in part by the National Natural Science Foundation of China (grant nos. 61101074 and 61372098).

7 References

1 Nicholson, D.L.: 'Spread spectrum signal design-LPE & AJ systems' (Computer Science Press, 1988)
2 Shiu, Y.-S., Chang, S.Y., Wu, H.-C., *et al.*: 'Physical layer security in wireless networks: a tutorial', *IEEE Wirel. Commun.*, 2011, **18**, (2), pp. 66–74
3 Narayanan, R.M., Chuang, J.: 'Covert communications using heterodyne correlation random noise signals', *Electron. Lett.*, 2007, **43**, (22), pp. 1211–1212
4 Chuang, J., DeMay, M.W., Narayanan, R.M.: 'Design, analysis, and performance of a noise modulated covert communications system', *EURASIP J. Wirel. Commun. Netw.*, 2008, **2008**, pp. 1–12
5 Blunt, S.D., Stiles, J., Allen, C., *et al.*: 'Diversity aspects of radar-embedded communications'. Proc. of Int. Conf. on Electromagnetics in Advanced Applications, 17–21 September 2007, pp. 439–442
6 Blunt, S.D., Yatham, P., Stiles, J.: 'Intrapulse radar-embedded communications', *IEEE Trans. Aerosp. Electron. Syst.*, 2010, **46**, (3), pp. 1185–1200
7 Axline, R.M., Sloan, G.R., Spalding, R.E.: 'Radar transponder apparatus and signal processing technique'. US Patent 5,486,830 23 January 1996
8 Hounam, D., Wagel, K.H.: 'A technique for the identification and localization of SAR targets using encoding transponders', *IEEE Trans. Geosci. Remote Sens.*, 2001, **39**, (1), pp. 3–7
9 Richardson, D.L., Stratmoen, S.A., Bendor, G.A., *et al.*: 'Tag communication protocol and system'. US Patent 6,329,944, 11 December 2001
10 Axline, R.M., Sloan, G.R., Spalding, R.E.: 'Transponder data processing methods and systems'. US Patent 6,577,266, 10 June 2003
11 Ormesher, R.C., Axline, R.M.: 'Methods and system suppressing clutter in a gain-block, radar-responsive tag system'. US Patent 7,030,805, 18 April 2006
12 Blunt, S.D., Yantham, P.: 'Waveform design for radar-embedded communications'. Proc. of Int. Waveform Diversity and Design Conf., June 2007, pp. 214–218
13 Metcalf, J., Blunt, S.D., Perrins, E.: 'Detector design and intercept metrics for intra-pulse radar-embedded communications'. The 2011 Military Communication Conf., pp. 188–192
14 Blunt, S.D., Metcalf, J., Biggs, C., *et al.*: 'Performance characteristics and metrics for intra-pulse radar-embedded communications', *IEEE J. Sel. Areas Commun.*, 2011, **29**, (10), pp. 2057–2066
15 Blunt, S.D., Biggs, C.: 'Practical considerations for intra-pulse radar-embedded communications'. 2009 Int. Waveform Diversity and Design Conf., February 2009, pp. 244–248
16 Blunt, S.D., Metcalf, J.: 'Using time reversal of multipath for intra-pulse radar-embedded communications'. 2010 Int. Waveform Diversity and Design Conf. (WDD), August 2010, pp. 155–158

8 Appendix

Similar with the procedure in [13, 14], the processing gain is defined as the ratio of the SINR after receive processing to the SINR before receiver processing, i.e.

$$\Delta \doteq \frac{\text{SINR}_o}{\text{SINR}_i} \tag{28}$$

Assume that the noise and clutter are uncorrelated, the SINR before processing can be found from

$$\begin{aligned} E\left[\|\boldsymbol{y}\|^2\right] &= E\left[\boldsymbol{y}^{\text{H}}\boldsymbol{y}\right] = E\left[(\boldsymbol{Sx} + \alpha\boldsymbol{c}_k + \boldsymbol{u})^{\text{H}}(\boldsymbol{Sx} + \alpha\boldsymbol{c}_k + \boldsymbol{u})\right] \\ &= E\left[\boldsymbol{x}^{\text{H}}\boldsymbol{S}^{\text{H}}\boldsymbol{Sx}\right] + E\left[|\alpha|^2\boldsymbol{c}_k^{\text{H}}\boldsymbol{c}_k\right] + E\left[\boldsymbol{u}^{\text{H}}\boldsymbol{u}\right] \end{aligned} \tag{29}$$

Using (6) and (7) and observing that the symbol is purely deterministic, the symbol power before processing becomes

$$S_i = |\alpha|^2 \boldsymbol{c}_k^{\mathrm{H}} \boldsymbol{c}_k = |\alpha|^2 \boldsymbol{b}_k^{\mathrm{H}} \boldsymbol{V}_{\mathrm{ND}} \boldsymbol{V}_{\mathrm{ND}}^{\mathrm{H}} \boldsymbol{V}_{\mathrm{ND}} \boldsymbol{V}_{\mathrm{ND}}^{\mathrm{H}} \boldsymbol{b}_k \tag{30}$$

where $\boldsymbol{b}_k = \boldsymbol{d}\beta_k$ and $\|\boldsymbol{d}\|^2 = 1$, so $\|\boldsymbol{b}_k\|^2 = 1$. Using $\boldsymbol{P} = \boldsymbol{V}_{\mathrm{ND}} \boldsymbol{V}_{\mathrm{ND}}^{\mathrm{H}}$, idempotent ($\boldsymbol{PP} = \boldsymbol{P}$) and Hermit ($\boldsymbol{P}^{\mathrm{H}} = \boldsymbol{P}$) properties of the projection matrix, the received signal power S_i can be simplified is

$$\begin{aligned} S_i &= |\alpha|^2 \boldsymbol{c}_k^{\mathrm{H}} \boldsymbol{c}_k = |\alpha|^2 \boldsymbol{b}_k^{\mathrm{H}} \boldsymbol{V}_{\mathrm{ND}} \boldsymbol{I} \boldsymbol{V}_{\mathrm{ND}}^{\mathrm{H}} \boldsymbol{b}_k \\ &= |\alpha|^2 \boldsymbol{b}_k^{\mathrm{H}} \boldsymbol{V}_{\mathrm{ND}} \boldsymbol{V}_{\mathrm{ND}}^{\mathrm{H}} \boldsymbol{b}_k \cong |\alpha|^2 (\boldsymbol{NM} - m)/\boldsymbol{NM} \end{aligned} \tag{31}$$

Using (29) and assuming all samples of the clutter are i.i.d., the interference power before processing is

$$\begin{aligned} R_i &= E[\boldsymbol{x}^{\mathrm{H}} \boldsymbol{S}^{\mathrm{H}} \boldsymbol{S} \boldsymbol{x}] \\ &= E[\mathrm{tr}\{\boldsymbol{S} \boldsymbol{x} \boldsymbol{x}^{\mathrm{H}} \boldsymbol{S}^{\mathrm{H}}\}] \\ &= \mathrm{tr}\{\boldsymbol{S} E[\boldsymbol{x}\boldsymbol{x}^{\mathrm{H}}] S^{\mathrm{H}}\} \\ &= \sigma_x^2 \mathrm{tr}\{\boldsymbol{S}\boldsymbol{S}^{\mathrm{H}}\} = \sigma_x^2 \mathrm{tr}\{\boldsymbol{V}\boldsymbol{\Lambda}\boldsymbol{V}^{\mathrm{H}}\} = \sigma_x^2 \mathrm{tr}\{\boldsymbol{\Lambda}\} \end{aligned} \tag{32}$$

where $\mathrm{tr}\{\bullet\}$ is the trace operation. As noise is assumed to be AWGN, the noise power is

$$N_i = E[u^{\mathrm{H}} u] = \sigma_u^2 \boldsymbol{NM} \tag{33}$$

The SINR after processing is found from

$$\begin{aligned} E[|\boldsymbol{w}_k^{\mathrm{H}} \boldsymbol{y}|^2] &= E[(\boldsymbol{w}_k^{\mathrm{H}} \boldsymbol{y})^{\mathrm{H}} (\boldsymbol{w}_k^{\mathrm{H}} \boldsymbol{y})] = E[\boldsymbol{y}^{\mathrm{H}} \boldsymbol{w}_k \boldsymbol{w}_k^{\mathrm{H}} \boldsymbol{y}] \\ &= \delta^{-2} E[\boldsymbol{y}^{\mathrm{H}} \boldsymbol{c}_k \boldsymbol{c}_k^{\mathrm{H}} \boldsymbol{y}] \\ &= \delta^{-2} E[(\boldsymbol{S}\boldsymbol{x} + \alpha \boldsymbol{c}_k + \boldsymbol{u})^{\mathrm{H}} \boldsymbol{c}_k \boldsymbol{c}_k^{\mathrm{H}} (\boldsymbol{S}\boldsymbol{x} + \alpha \boldsymbol{c}_k + \boldsymbol{u})] \end{aligned} \tag{34}$$

As the noise and clutter are independent from each other, all cross-correlation terms are zero. The resultant filtered, received signal magnitude can be separated into symbol S_o, interference R_o, and noise N_o terms as

$$E[|\boldsymbol{w}_k^{\mathrm{H}} \boldsymbol{y}|^2] = S_o + R_o + N_o \tag{35}$$

$$S_o = \delta^{-2} |\alpha|^2 \boldsymbol{c}_k^{\mathrm{H}} \boldsymbol{c}_k \boldsymbol{c}_k^{\mathrm{H}} \boldsymbol{c}_k \tag{36}$$

$$R_o = \delta^{-2} E[\boldsymbol{x}^{\mathrm{H}} \boldsymbol{S}^{\mathrm{H}} \boldsymbol{c}_k \boldsymbol{c}_k^{\mathrm{H}} \boldsymbol{S} \boldsymbol{x}] \tag{37}$$

$$N_o = \delta^{-2} E[\boldsymbol{u}^{\mathrm{H}} \boldsymbol{c}_k \boldsymbol{c}_k^{\mathrm{H}} \boldsymbol{u}] \tag{38}$$

Using (31) and (36), the symbol power after receiver filtering becomes

$$S_o = \delta^{-2} |\alpha|^2 (\mathbf{Pd})^{\mathrm{H}} \boldsymbol{c}_k \boldsymbol{c}_k^{\mathrm{H}} \mathbf{Pd} = \delta^{-2} |\alpha|^2 (\boldsymbol{NM} - m)^2 / (\boldsymbol{NM})^2 \tag{39}$$

Using (37) and the identity $E[\boldsymbol{a}^{\mathrm{H}} \boldsymbol{a}] = E[\mathrm{tr}\{\boldsymbol{a}\boldsymbol{a}^{\mathrm{H}}\}]$ for a some arbitrary vector, the interference power after receive filtering can be given as

$$\begin{aligned} R_o &= \delta^{-2} \sigma_x^2 \mathrm{tr}\{\boldsymbol{d}^{\mathrm{H}} \boldsymbol{V}_{\mathrm{ND}} \boldsymbol{V}_{\mathrm{ND}}^{\mathrm{H}} \boldsymbol{V} \boldsymbol{\Lambda} \boldsymbol{V}^{\mathrm{H}} \boldsymbol{V}_{\mathrm{ND}} \boldsymbol{V}_{\mathrm{ND}}^{\mathrm{H}} \boldsymbol{d}\} \\ &= \delta^{-2} \sigma_x^2 \mathrm{tr}\{\boldsymbol{\gamma}_{\mathrm{ND}}^{\mathrm{H}} \boldsymbol{\Lambda}_{\mathrm{ND}} \boldsymbol{\gamma}_{\mathrm{ND}}\} \\ &\cong \delta^{-2} \sigma_x^2 \mathrm{tr}\{\boldsymbol{\Lambda}_{\mathrm{ND}}\} / \boldsymbol{NM} \end{aligned} \tag{40}$$

by using the unit norm constraint on $\boldsymbol{b}_k$. Finally, the noise power after receive processing simplifies to

$$\begin{aligned} N_o &= \delta^{-2} E[\boldsymbol{u}^{\mathrm{H}} \mathbf{Pd} (\mathbf{Pd})^{\mathrm{H}} \boldsymbol{u}] \\ &= \delta^{-2} E[\mathrm{tr}\{(\mathbf{Pd})^{\mathrm{H}} \boldsymbol{u}\boldsymbol{u}^{\mathrm{H}} \mathbf{Pd}\}] \\ &= \delta^{-2} \sigma_u^2 \mathrm{tr}\{(\mathbf{Pd})^{\mathrm{H}} \mathbf{Pd}\} \\ &= \delta^{-2} \sigma_u^2 \boldsymbol{d}^{\mathrm{H}} \boldsymbol{V}_{\mathrm{ND}} \boldsymbol{V}_{\mathrm{ND}}^{\mathrm{H}} \boldsymbol{V}_{\mathrm{ND}} \boldsymbol{V}_{\mathrm{ND}}^{\mathrm{H}} \boldsymbol{d} \\ &= \delta^{-2} \sigma_u^2 \boldsymbol{\gamma}_{\mathrm{ND}}^{\mathrm{H}} \boldsymbol{\gamma}_{\mathrm{ND}} \\ &= \delta^{-2} \sigma_u^2 (\boldsymbol{NM} - m)/\boldsymbol{NM} \end{aligned} \tag{41}$$

For an arbitrary radar waveform and using (31)–(33) the SINR before receiver processing is

$$\mathrm{SINR}_i = \frac{|\alpha|^2 (\boldsymbol{NM} - m)}{\sigma_x^2 \mathrm{tr}\{\Lambda\} + \sigma_u^2 (\boldsymbol{NM})} \tag{42}$$

Using (39)–(41), the SINR after receive processing with the decorrelating filter is

$$\mathrm{SINR}_o = \frac{|\alpha|^2 (\boldsymbol{NM} - m)^2}{\sigma_x^2 \mathrm{tr}\{\boldsymbol{\Lambda}_{\mathrm{ND}}\} + \sigma_u^2 (\boldsymbol{NM} - m)} \tag{43}$$

The processing gain parameterized by the dominant subspace dimensionality m is

$$\Delta(m) = \frac{\mathrm{SINR}_o}{\mathrm{SINR}_i} = \frac{(\boldsymbol{NM} - m)(\sigma_x^2 \mathrm{tr}\{\boldsymbol{\Lambda}_{\mathrm{ND}}\} + \sigma_u^2 \boldsymbol{NM})}{\sigma_x^2 \mathrm{tr}\{\boldsymbol{\Lambda}_{\mathrm{ND}}\} + \sigma_u^2 (\boldsymbol{NM} - m)} \tag{44}$$

If the radar waveform is constant modulus, (44) simplifies to

$$\Delta(m) = \frac{\boldsymbol{NM}(\boldsymbol{NM} - m)(\sigma_x^2 + \sigma_u^2)}{\sigma_x^2 \mathrm{tr}\{\boldsymbol{\Lambda}_{\mathrm{ND}}\} + \sigma_u^2 (\boldsymbol{NM} - m)} \tag{45}$$